148 WET MICROBURST EVENTS OBSERVED WITH PHASED ARRAY RADAR

Arthur Witt[1,*], Travis M. Smith[1,2], Pamela L. Heinselman[1], Steven T. Irwin[2], and Kevin L. Manross[3]
[1] NOAA/National Severe Storms Laboratory
[2]Cooperative Institute for Mesoscale Meteorological Studies, The University of Oklahoma, Norman, Oklahoma
[3]National Center for Atmospheric Research, Boulder, Colorado

1. INTRODUCTION

Though downbursts were thought to exist as early as the 1930's (Fujita and Wakimoto 1981), it wasn't until their dangerous impact on aviation was discovered that research on this phenomenon began to flourish (Fujita 1980). Fujita (1981) quantitatively defines a microburst as a downburst occurring on a horizontal scale from 0.4 – 4 km. Several years later, Wilson et. al. (1984) developed a radar-based definition of a microburst, using C and S-band Doppler radar data collected during the Joint Airport Weather Studies (JAWS) Project (McCarthy et al. 1982). Wilson et al. (1984) defined a microburst as a diverging Doppler velocity signature having a velocity differential of 10 m s^{-1} within a 4-km horizontal distance. For real-time operational warnings to the aviation community, the automated microburst prediction algorithm (Wolfson et al. 1994) issues microburst alerts when a velocity differential of 15 m s^{-1} or higher within a 4-km horizontal distance is identified ("wind-shear alerts" are issued if the velocity differential is between 7.5 – 15 m s^{-1}).

Microbursts are known to occur in a variety of atmospheric environments. However, the physical processes leading to the occurrence of a microburst can vary greatly depending on the character of the atmospheric environment. Results from the JAWS Project (McCarthy et al. 1982) reveal that some microbursts are accompanied by heavy precipitation from thunderstorms, whereas others are associated with virga shafts from a variety of high-based clouds. This distinction has led to microbursts being classified into two broad categories: "dry" and "wet." Dry microbursts are defined as microbursts accompanied by little or no precipitation at the ground between the onset and end of the high surface winds, and are most often observed in higher terrain regions (Fujita 1985; Wakimoto 1985). The typical environment favoring dry microbursts is characterized in the morning by a radiation inversion (40– 50 mb deep) capped by a dry adiabatic layer that extends up to a mid-altitude of ~500 mb (Wakimoto 1985). By afternoon, the inversion is replaced by a shallow, super-adiabatic layer (<10 mb deep) near the surface. Generally, the surface is relatively dry and a nearly saturated layer exists ~500 mb. The moisture profile from the surface to 500 mb is usually "well-mixed" with a constant or increasing mixing ratio. The clouds producing dry microbursts tend to have relatively high bases above ground level, with the strong surface winds resulting from negative buoyancy generated by evaporation, melting, and/or sublimation of precipitation below cloud base (Hjelmfelt 1987; Srivastava 1987; Proctor 1989). In contrast, "wet" microbursts predominate in environments typically characterized by shallow sub-cloud layers, warmer cloud bases, and vertical thermodynamic profiles that are more humid (Wakimoto and Bringi 1988; Kingsmill and Wakimoto 1991; Atkins and Wakimoto 1991). Atkins and Wakimoto (1991) found that wet microbursts were more likely on days when $\Delta\theta_e$ > 20 K versus $\Delta\theta_e$ < 13 K on days with thunderstorms and no microbursts.[1] Proctor (1989) found via numerical model sensitivity studies that the intensity and likelihood of wet microbursts increase as the environmental lapse rate becomes steeper, the melting level becomes higher above ground level, and the humidity becomes drier near the melting level and more moist at low altitudes. This study focuses on wet microbursts, as these are the type that thus-far occurred when PAR data were collected.

Microbursts are quickly evolving phenomena that usually form and dissipate within 20 min (Fujita 1981; Wilson et. al. 1984; Hjelmfelt 1988). Since microbursts can develop rapidly, often in less than 5 min, they are challenging to predict. Hence, several previous studies attempted to identify reliable precursors to microbursts in an effort to forecast these small-scale phenomena. In their analysis of multiple-Doppler radar data of microburst-producing storms in Colorado, Roberts and Wilson (1989) found several precursors of microbursts related to the vertical profiles of reflectivity and convergence in the storm. Proctor (1989) showed that with an increase in the diameter of the downdraft resulting from increasing width of precipitation shafts, the peak outflow speeds of the microburst, the depth of the outflow and the height of the outflow peak all increase, but the mean horizontal wind shear decreases.

*Corresponding author address: Arthur Witt, NSSL, 120 David L. Boren Blvd., Norman, OK 73072. E-mail: Arthur.Witt@noaa.gov.

[1] $\Delta\theta_e = \theta_{emax} - \theta_{emin}$. θ_{emax} refers to the maximum value of θ_e found at or just above round level.

Microburst nowcasting algorithms have been created to assist forecasters with identifying microburst-producing storms. One of these algorithms is the Damaging Downburst Prediction and Detection Algorithm (DDPDA), which was designed for use by the WSR-88D system (Smith et al. 2004). The DDPDA utilizes 26 reflectivity and radial velocity-based parameters, several in combination with environmental data, to discriminate between severe downburst-producing storm cells and cells not expected to produce a strong outflow.[2] Initial testing of the DDPDA indicated moderate skill, with a median Heidke skill score (HSS) of 0.40 and median lead time of 5.5 min in the 20 – 45 km range from the radar and median HSS of 0.17 and median lead time of 0 min in the 45 – 80 km range. At airports with a Terminal Doppler Weather Radar (TDWR), microburst detection and prediction is done via the Integrated Terminal Weather System (ITWS; Wolfson 1994). The Microburst Prediction Algorithm (MPA) in ITWS focuses on thunderstorm evolution and downdraft development using machine-intelligent image processing and data-fusion techniques. The algorithm also uses temperature/humidity data to aid in predicting a microburst's peak outflow strength. Initial testing of the MPA was done in two modes: a restricted mode to minimize false predictions of microbursts (requires a wind-shear alert prior to a microburst alert) and an unrestricted mode to maximize probability of predicting microbursts and lead times. Test results for the unrestricted mode were an average probability of prediction (POP) of 72% and average lead time of 226 s, with a probability of false prediction (PFP) of 27%. For the restricted mode, the results were an average POP of 68% and average lead time of 92 s, with a PFP of 0%. Though all the above mentioned precursors and prediction schemes can be useful, they are dependent on sufficient lead time of the necessary observations, particularly for the radar-based parameters.

Although users of operational radar data list as one of their top priorities faster update times (LaDue et al. 2010), currently the fastest full volume scan available on the operational WSR-88D is with VCP 12/212, which completes a volume scan in approximately 4.2 min (Brown et al. 2005).[3] The TDWR completes volume scans slightly faster than the WSR-88D (although at lower vertical resolution), with an average scan time of around 2–3 min (Wolfson 1994). However, this volume scan time is still more than double the typical volume scan time used by the phased array radar (PAR; 1 min or less). Heinselman et al. (2008) analyzed a single microburst comparing the PAR with the KTLX WSR-88D. Analysis of this microburst showed that the faster volume scan times offered by the PAR gave better visibility of microburst precursors compared to KTLX. Since then, additional data collection by the PAR on microburst-producing storms provides us the opportunity to expand on this initial single observation, broadening the analysis of the potential improvements the PAR might provide for more timely and accurate prediction of microbursts.

2. METHODS

2.1 Inclusion criteria for storms

Since microburst outflows are relatively shallow phenomena, with typical depths of ~250 – 750 m (Hjelmfelt 1988; Proctor 1989), the maximum radial range of the study area was limited to 60 km, the maximum distance these depths can be observed at the lowest elevation scan. Since this study focuses on wet microbursts, all candidate storms needed to attain a maximum reflectivity value of 55 dBZ or higher, and be sampled by the PAR at least 10 min prior to the initial time of microburst observation, to allow for adequate measurement of precursors.

Storms were determined to be microburst-producing based on the maximum strength of observed low-altitude divergent outflow signatures from the PAR radial velocity data. Outflow magnitudes were calculated for each divergent signature using a linear least squares derivative (LLSD) of the radial velocity field as outlined by Smith and Elmore (2004). The process involved initially calculating the radial divergence from the base velocity data (e.g., Fig. 1) and then mapping it to a 3D latitude-longitude-height grid with a resolution of 0.005° x 0.005° x 0.5 km (Lakshmanan et al 2006) (e.g., Fig. 2). The outflows were then categorized as a microburst if the peak divergence within the signature during the life-cycle of the outflow was 0.0025 s^{-1} or higher [equivalent to $\Delta V_r \geq 10$ m s^{-1} over a radial distance (Δr) of 4 km] on at least one grid point at the 0.5 km vertical height (above radar level). Outflows with peak divergence values lower than 0.0025 s^{-1} were categorized as non-microburst strength.

[2]Smith et al. (2004) defined a severe downburst by one or more of the following criteria: a measured wind gust of 50 kt at the surface; wind damage recorded in Storm Data or storm spotter logs; a radar-measured wind of 25 m s^{-1} or a divergence signature with a radial velocity difference greater than 40 m s^{-1} within 1 km of the surface.

[3]However, the Automated Volume Scan Evaluation and Termination (AVSET) function on the WSR-88D can reduce the volume scan time of VCP-12/212 down to as short as 190 s (Chrisman 2009).

2.2 Data cases

The data set for this study included a total of 25 storms meeting the inclusion criteria occurring on eight days when PAR data were collected (Table 1). Seventeen of the 25 storms produced moderately strong microbursts having observed maximum low-altitude divergence values between 0.0025 s^{-1} and 0.0035 s^{-1}, with eight storms producing very strong microbursts having observed maximum low-altitude divergence values higher than 0.0035 s^{-1}. The thermodynamic environment for each day in the data set was similar to previous studies of wet microbursts (e.g., $\Delta\theta_e$ > 20 K; Atkins and Wakimoto 1991). Mean winds varied from nearly calm on 29 August 2008 to moderately-strong from a southwesterly to northwesterly direction on the other days. The lower wind speeds on 29 August 2008 may be one reason why the storms on this day were generally weaker than the storms on the other days (data on each storm's strength is shown in section 3).

2.3 Parameters analyzed as microburst precursors

Given the small size of the data set, we chose to limit our analysis to a few select parameters based on the primary downdraft forcing mechanisms associated with wet microbursts, namely precipitation drag and cooling from melting ice (predominately hail) (Roberts and Wilson 1989). The first parameter focuses on the storm's precipitation core, which for this study is the volume of 55-dBZ or higher reflectivity echo (Z_{55}). The decision to use Z_{55} for defining the precipitation core is based primarily on the importance of hail within the core as a source of the negative buoyancy driving the downdraft that ultimately produces the microburst at the surface (Srivastava 1987; Proctor 1989), with 55 dBZ often used as the reflectivity threshold defining the hail versus liquid-water regions of the storm (Liu and Chandrasekar 2000). A secondary reason for choosing 55 dBZ is that past observational studies have used this reflectivity value in their analysis of microburst-producing storms, e.g., for categorizing microbursts as low, moderate or high reflectivity events (Roberts and Wilson 1989), or for defining the main precipitation core of storms producing wet microbursts (Atkins and Wakimoto 1991). The specific aspects of the core that were analyzed via this parameter were it's depth and minimum height (i.e., the core's vertical extent). The depth served as a simple measure of the core intensity, with time-trends in the minimum height of the core being important for determining the likely occurrence and timing of the low-altitude divergent outflow (e.g., whether or not the core is descending in height). Since the intensity and height trends in a storm's precipitation core may not be accurately indicated solely via the 55-dBZ reflectivity level, two additional reflectivity levels are used: 60 dBZ (Z_{60}) and 65 dBZ (Z_{65}). Core heights were determined by first mapping the radar reflectivity data to the same 3D latitude-longitude-height grid used for calculating divergence. Then, the core depth was calculated by summing the number of grid points in each vertical column having reflectivity greater than or equal to 55 dBZ, 60 dBZ and 65 dBZ (e.g., Fig. 3). These grid-point sums were subsequently divided by 2 (since the vertical grid resolution used here was 0.5 km) to obtain the final depth values.

The second parameter analyzed was the peak mid-altitude (2 – 6 km ARL) convergence associated with the storm's precipitation core (Roberts and Wilson 1989). The peak mid-altitude convergence was determined using the 3D latitude-longitude-height grid of LLSD derived divergence calculations, initially generating a 2D grid of the maximum convergence in the vertical column for the grid heights of 2 – 6 km (e.g., Fig. 4), with the peak mid-altitude convergence then being the highest of these convergence values in the area linked to the storm's precipitation core (e.g., the white circle in Fig. 4). However, in single-radar observations, convergence alone is not a reliable precursor to microburst formation, as the sign of the associated vertical motion is ambiguous. But, previous studies have noted that when increasing mid-altitude convergence is co-located with a descending precipitation core, formation of a downdraft is likely (Roberts and Wilson 1989). Also, microbursts usually coincide temporally and spatially with the arrival of descending precipitation cores near the surface (Roberts and Wilson 1989; Atkins and Wakimoto 1991). Hence, for a particular peak mid-altitude convergence value to qualify as a microburst precursor, it must occur in combination with a descending precipitation core. For this study, the minimum height of the precipitation core (subsequently referred to as the "base" height) was determined via the lowest altitude of Z_{55}, Z_{60} and Z_{65}. The core was defined as descending if the base height of Z_{55}, Z_{60} or Z_{65} decreased by at least 1 km from the maximum base height (for that reflectivity threshold), provided that the maximum base height was 2 km or higher (corresponding to the lowest height used for determining the peak mid-altitude convergence).

3. RESULTS AND DISCUSSION

The ability of the PAR to rapidly scan in high resolution the full 3D volume of a storm allows for examination in much finer detail the temporal patterns of the precursor parameters than would be possible from the operational weather radars. Hence, for each of the 25 microburst-producing storms, the temporal patterns of the precursor parameters were examined via time-series graphs of the storm's core base height, core top height, and maximum mid-altitude convergence. The time period analyzed was from the initial observation of

the microburst near the surface to a maximum of 17 min prior to the initial observation of the microburst.[4] For several of the weaker storms, the time interval was less than 17 min, extending back to either the first observation of 55 dBZ or higher reflectivity, or the maximum mid-altitude convergence exceeded 0.002 s^{-1}. Although substantial variations in the magnitude and trend patterns of the precursor parameters existed for the 25 storms, it was possible to subjectively categorize them into several distinct groups, based on the degree that their patterns matched the expected characteristics of microburst-producing storms from past research (Table 2). Group 1 contained storms (N=9) having the best match of characteristics, namely an intense, descending precipitation core associated with moderate to strong mid-altitude convergence (at least three observations with values of 0.003 s^{-1} or higher) (Fig. 5). Group 2 contained storms (N=4) having moderate to strong mid-altitude convergence and an intense, descending precipitation core, but the core remained somewhat elevated (base core height remained at mid-altitudes) (Fig. 6). Group 3 contained storms (N=5) having moderate to strong mid-altitude convergence, but the precipitation core did not notably descend (Fig. 7). Group 4 included those storms with only weak mid-altitude convergence (less than three observations with values of 0.003 s^{-1} or higher) (Fig. 8). Group 5 contained the remaining storms, all with relatively weak precipitation cores (maximum reflectivity less than 60 dBZ) (Fig. 9). Several storms in Groups 4 and 5 (27 Apr 2009 – #2; 29 Aug 2008 – #5; 29 Aug 2008 – #7) could have been put in either group. The 27 Apr 2009 – #2 and 29 Aug 2008 – #5 storms were put in Group 4 because they had the weakest mid-altitude convergence patterns, and the 29 Aug 2008 – #5 storm was put in Group 5 because it had the 2nd weakest precipitation core.

A majority of the storms analyzed had all (Group 1) or most (Group 2) of the typical precursor characteristics associated with wet microbursts. The precursor most frequently observed was moderate to strong mid-altitude convergence (20 storms). However, there was no consist pattern in the time trends of mid-altitude convergence, although several storms did have a substantial increase in the magnitude of mid-altitude convergence just prior to microburst occurrence (e.g., 31 Aug 2010 – #1; 16 Jul 2009 – #2). This suggests that once sufficiently strong mid-altitude convergence is observed (to support downdraft development), microburst occurrence becomes more dependent on descent of the precipitation core toward the surface. But as is evident from the number of storms in Group 3, microbursts also occur without a distinctly descending core, indicating the importance of multiple precursor parameters for identifying microburst-producing storms. In terms of microburst intensity, the average and median maximum low-altitude divergence was highest for Group 1, somewhat lower for Groups 2, 3 and 5, and lowest for Group 4 (Table 2).

Beyond the initial results presented here, future project plans include comparing the magnitude and time-series trend patterns of microburst-producing storms with high-reflectivity storms that did not produce microbursts. Different methods of measuring the precursor parameters, such as volumetric versus single grid point or vertical column values, will be evaluated. Also, the potential benefits of high temporal PAR observations versus the slower update rates of operational weather radars will be examined.

4. ACKNOWLEDGEMENTS

Partial funding of this project was provided by the NOAA/Office of Oceanic and Atmospheric Research under NOAA–University of Oklahoma Cooperative Agreement #NA11OAR4320072, U.S. Department of Commerce (DOC). The statements, findings, conclusions, and recommendations are those of the authors and do not necessarily reflect the views of NOAA or the U.S. DOC.

5. REFERENCES

Atkins, N. T., and R. Wakimoto, 1991: Wet microburst activity over the southeastern United States: Implications for forecasting. *Wea. Forecasting,* **6,** 470–482.

Atlas, D., C. W. Ulbrich, and C. R. Williams, 2004.: Physical origin of a wet microburst: observations and theory. *J. Atmos. Sci.,* **61,** 1186–1196.

Brown, R. A., V. T. Wood, R. M. Steadman, R. R. Lee, B. A. Flickinger, and D. Sirmans, 2005: New WSR-88D volume coverage pattern 12: Results of field tests. *Wea. Forecasting*, **20,** 385–393.

Chrisman, J. N., 2009: Automated volume scan evaluation and termination (AVSET): A simple technique to achieve faster volume scan updates for the WSR-88D. *34th Conf. on Radar Meteor.* Williamsburg, Amer. Meteor. Soc., P4.4.

[4] Seventeen minutes corresponds to the typical time period of four full WSR-88D volume scans when using volume-coverage-pattern 12. Future analysis will investigate the advantages of rapidly-updating PAR data versus the slower update rates of operational weather radars.

Fujita, T. T., 1980: Downbursts and microbursts - an aviation hazard. Preprints, *19th Conf. on Radar Meteorology,* Miami, 94-101.

Fujita, T. T., and R. Wakimoto, 1981: Five scales of airflow associated with a series of downbursts on 16 July 1980*. Mon. Wea. Rev.*, **109,** 1438–1456.

Fujita, T. T., 1985: The downburst. SMRP Research Paper 210, University of Chicago, 122 pp. [NTIS PB-148880.]

Hjelmfelt, M. R., 1987: The Microbursts of 22 June 1982 in JAWS. *J. Atmos. Sci.*, **44,** 1646–1665.

Hjelmfelt, M. R., 1988: Structure and life cycle of microburst outflows observed in Colorado. *J. Appl. Meteor.,* **27,** 900–927.

Heinselman, P. L., D. L. Priegnitz, K. L. Manross, T. M. Smith, and R. W. Adams, 2008: Rapid sampling of severe storms by the National Weather Radar Testbed phased array radar. *Wea. Forecasting,* **23,** 808–824.

Kingsmill, D. E., and R. M. Wakimoto, 1991: Kinematic, Dynamic, and Thermodynamic Analysis of a Weakly Sheared Severe Thunderstorm over Northern Alabama. *Mon. Wea. Rev.*, **119,** 262–297.

LaDue, D. S., P. L. Heinselman, and J. F. Newman, 2010: Strengths and limitations of current radar systems for two stakeholder groups in the Southern Plains. *Bull. Amer. Meteor. Soc.*, **91,** 899–910.

Lakshmanan, V, T. Smith, K. Hondl, G J. Stumpf, and A. Witt, 2006: A Real-Time, Three-Dimensional, Rapidly Updating, Heterogeneous Radar Merger Technique for Reflectivity, Velocity, and Derived Products. *Wea. Forecasting*, **21,** 802–823.

Liu, H., and V. Chandrasekar, 2000: Classification of hydrometeor based on polarimetric radar measurements: Dvelopment of fuzzy logic and neurofuzzy systems and in situ verification. J. Atmos. Oceanic Technol, vol.17, pp. 140–164, 2000.

Marzban, C., 1998: Scalar Measures of Performance in Rare-Event Situations.

Proctor, F. H., 1989: Numerical simulations of an isolated microburst. Part II: Sensitivity experiments. *J. Atmos. Sci.,* **46,** 2143–2165. *Wea. Forecasting,* **13,** 753-763.

Roberts, R. D., and J. Wilson, 1989: A proposed microburst nowcasting procedure using single-Doppler radar. *J. Appl. Meteor.,* **28,** 285–303.

Smith, T., and K. L. Elmore, 2004: The use of radial velocity derivatives to diagnose rotation and divergence. Preprints, *11th Conf. on Aviation, Range, and Aerospace*, Hyannis, MA, Amer. Meteor. Soc., CD-ROM, P5.6.

Smith, T. M., K. L. Elmore, and S. A. Dulin, 2004: A damaging downburst prediction and detection algorithm for the WSR-88D. *Wea. Forecasting,* **19**, 240–250.

Srivastava, R. C., 1987: A model of intense downdrafts driven by melting and evaporation of precipitation. *J. Atmos. Sci.*, **44,** 1752–1773.

Wakimoto, 1985: Forecasting dry microburst activity over the High Plains. *Mon. Wea. Rev.*, **113,** 1131-1143.

Wakimoto, R. M., and V. N. Bringi, 1988: Dual-Polarization observations of Microbursts Associated with Intense Convection: The 20 July Storm during the MIST Project. *Mon. Wea. Rev.*, **116,** 1521–1539.

Wilson, J. W., R. D. Roberts, C. Kessinger, and J. McCarthy, 1984: Microburst wind structure and evaluation of Doppler radar for airport wind shear detection. *J. Climate Appl. Meteor.,* **23,** 898–915.

Wolfson, M. M., R. L. Delanoy, B. E. Forman, R. G. Hallowell, M. L. Pawlak, and P. D. Smith, 1994: Automated microburst wind-shear prediction. *Linc. Lab J.,* **7,** 399–426.

Table 1. Number of microburst-producing storms analyzed for each day in the data set. Environmental values shown were derived from the 0000 UTC OUN sounding, except for 27 April 2009, where values are from the 1200 UTC OUN sounding. Here, $\Delta\theta_e$ is the difference between the surface θ_e and the minimum θ_e value in the lowest 400 mb AGL, and the mean wind [direction and speed (m s^{-1})] is in the layer from the lifted condensation level to the equilibrium level (the layer calculated by parcel theory to contain the thunderstorm updraft). The maximum low-altitude divergence values for each day correspond to consecutive microburst numerical labels (e.g., 29 Aug 2008 – #5 = 26).

Date	Storms with an observed microburst	Maximum low-altitude divergence (10^{-4} s^{-1}) for each microburst	$\Delta\theta_e$	Mean wind
9 Jul 2007	1	27	30	272 / 9
24 Aug 2007	3	29, 31, 33	22	252 / 13
29 Aug 2008	7	34, 30, 37, 35, 26, 25, 33	28	174 / 1
27 Apr 2009	2	32, 37	30	222 / 18
30 Jun 2009	3	61, 32, 39	25	320 / 8
16 Jul 2009	4	26, 42, 30, 42	31	301 / 10
26 Aug 2009	1	30	30	286 / 11
31 Aug 2010	4	30, 35, 43, 48	22	220 / 17

Table 2. Trend group characteristics and storms in each group.

Trend group	Characteristics	Storms in group	Average / median maximum low-altitude divergence (10^{-4} s^{-1})
1	Intense, descending core; moderate to strong mid-altitude convergence	31 Aug 2010 – #1, #4; 26 Aug 2009 – #1; 16 Jul 2009 – #2, #3; 30 Jun 2009 – #1, #2, #3; 29 Aug 2008 – #4	39 / 35
2	Moderate to strong mid-altitude convergence with a descending core, but the core base remains somewhat elevated	31 Aug 2010 – #2; 27 Apr 2009 – #1; 24 Aug 2007 – #2, #3	33 / 32
3	Moderate to strong mid-altitude convergence, but without a distinctly descending core	31 Aug 2010 – #3; 16 Jul 2009 – #1, #4; 24 Aug 2007 – #1; 9 Jul 2007 – #1	33 / 29
4	Weak mid-altitude convergence	27 Apr 2009 – #2; 29 Aug 2008 – #2, #5, #6	30 / 28
5	Relatively weak core (max Z < 60 dBZ)	29 Aug 2008 – #1, #3, #7	35 / 34

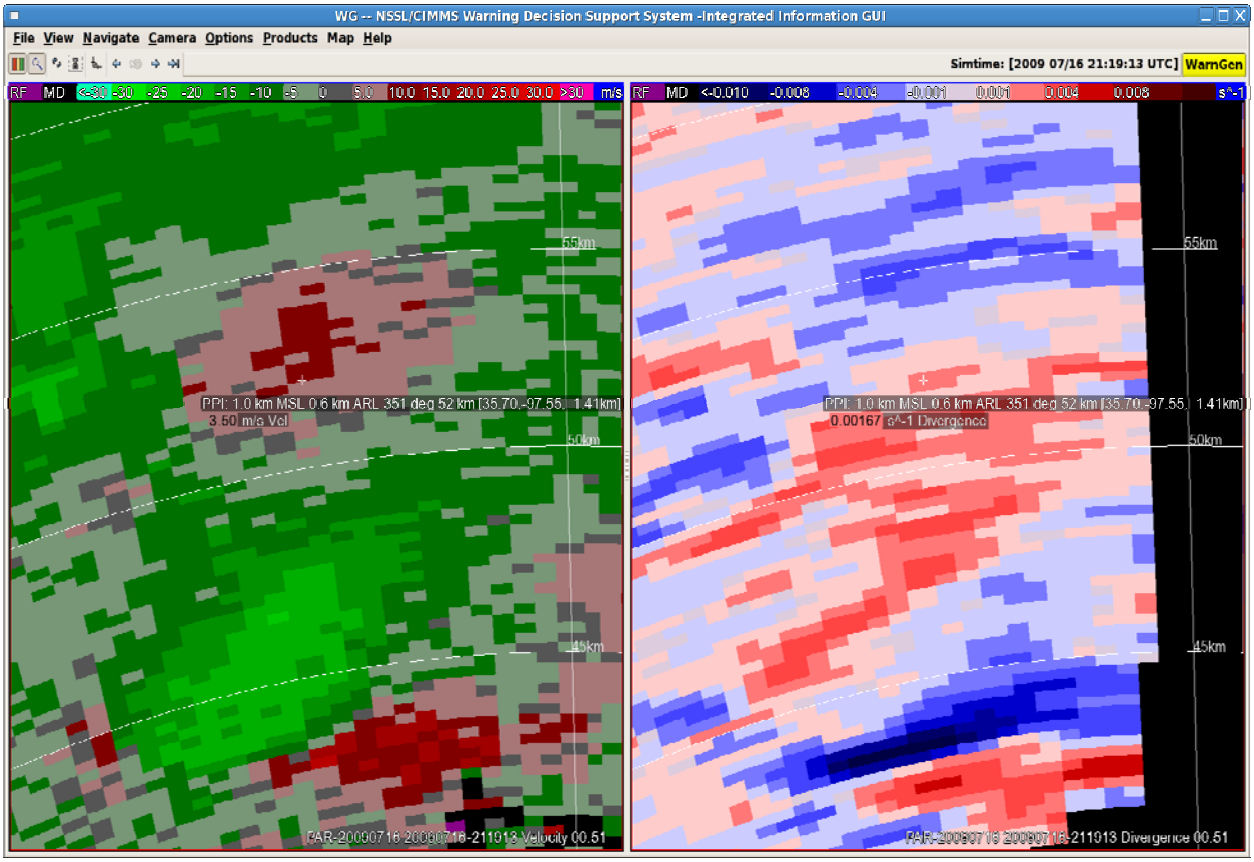

Figure 1. Example of radial divergence (right image) for a microburst on 16 July 2009 calculated using a linear least squares derivative of the radial velocity data (left image). Radar data are from the 0.5° elevation scan of the PAR at 21:19:13 UTC.

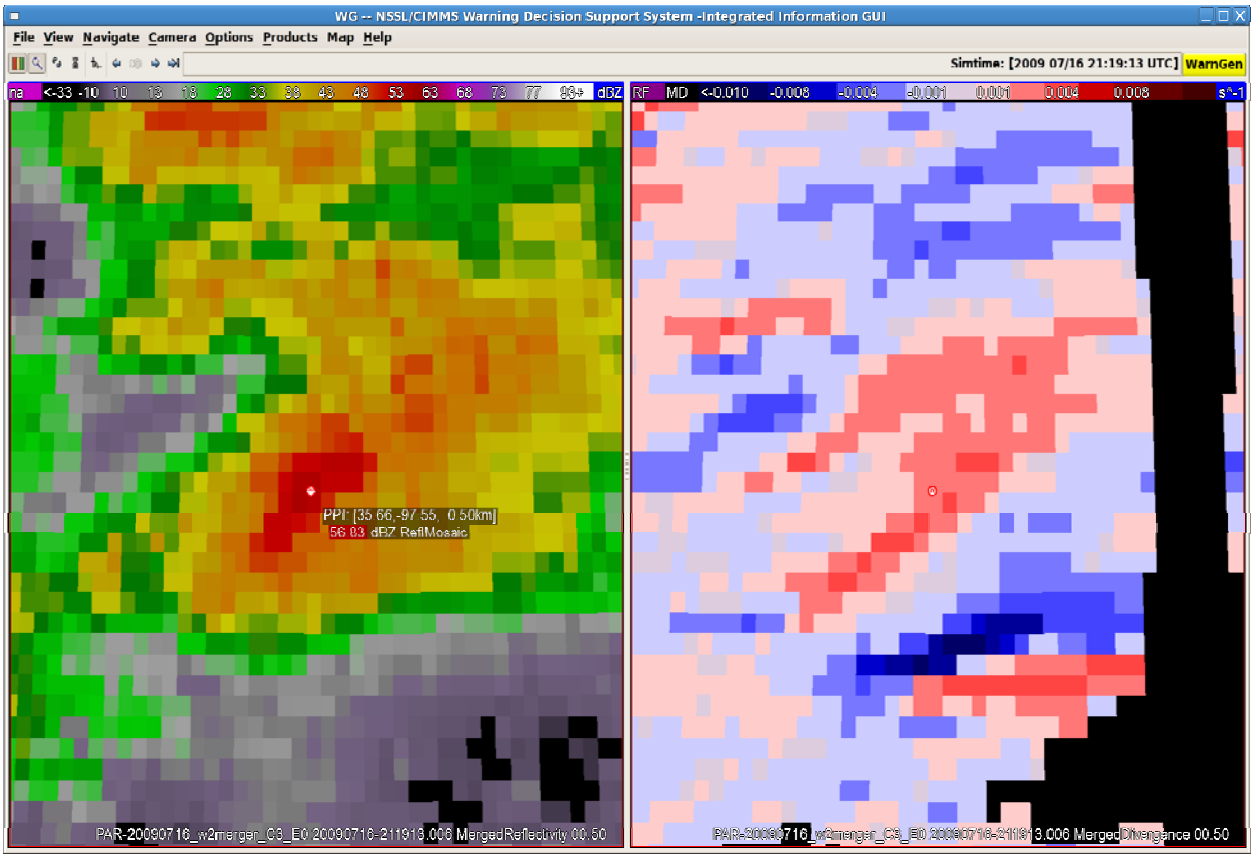

Figure 2. Example of grid-based radial divergence (right image) and reflectivity (left image) at the 0.5 km height level for the microburst shown in Fig. 2.

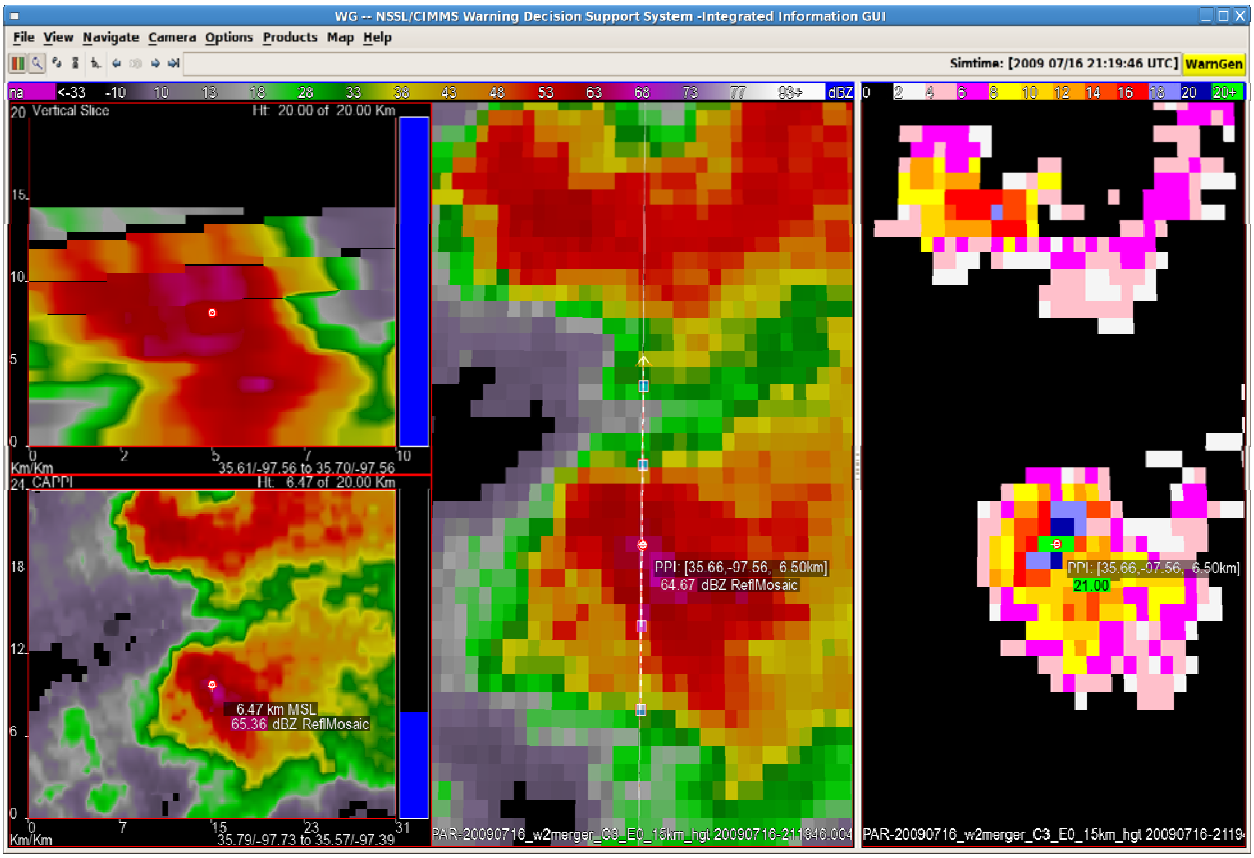

Figure 3. Example of the number of grid points in each vertical column having reflectivity 55 dBZ or higher (right image), along with corresponding vertical reflectivity cross-section (upper-left image) and horizontal reflectivity at the 6.5 km level (lower-left and middle images).

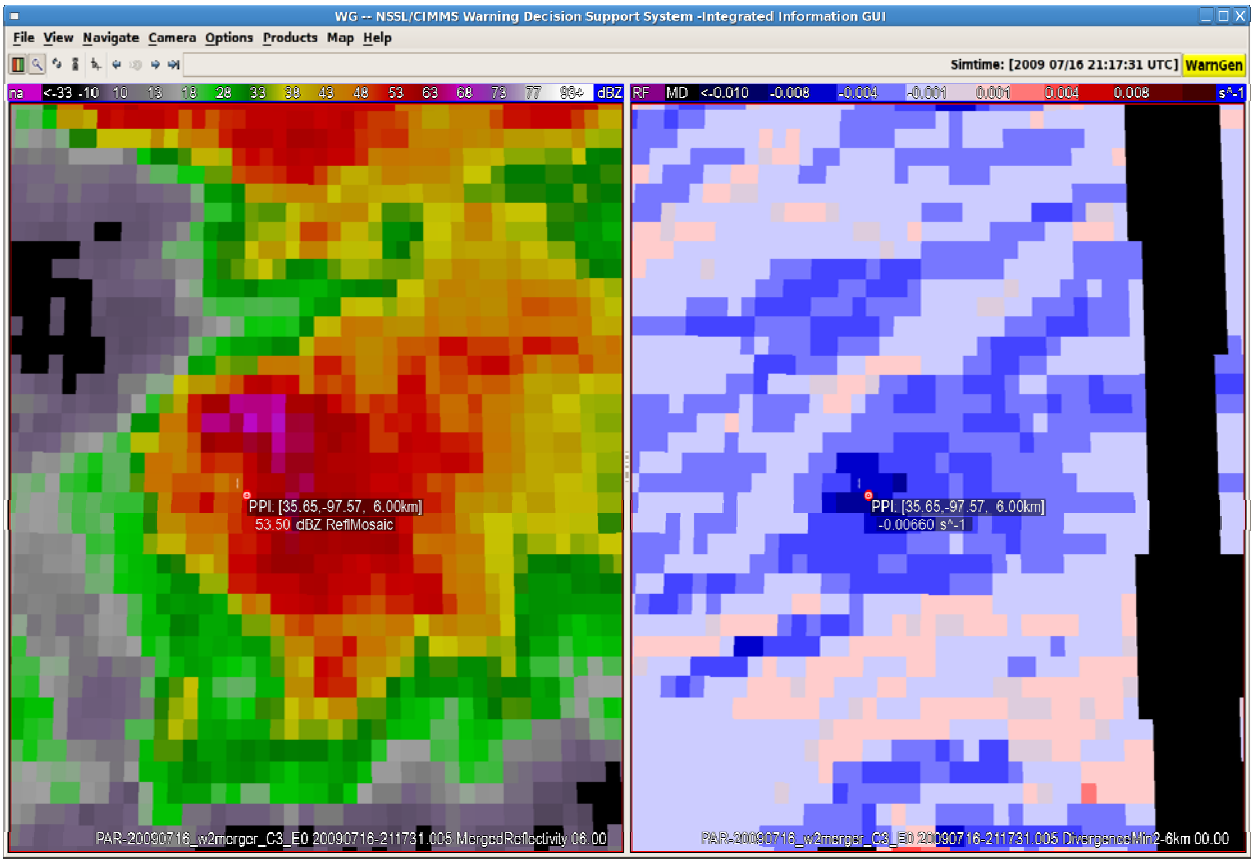

Figure 4. Example of peak mid-altitude convergence (right image) and reflectivity (left image) at the 6.0 km height level.

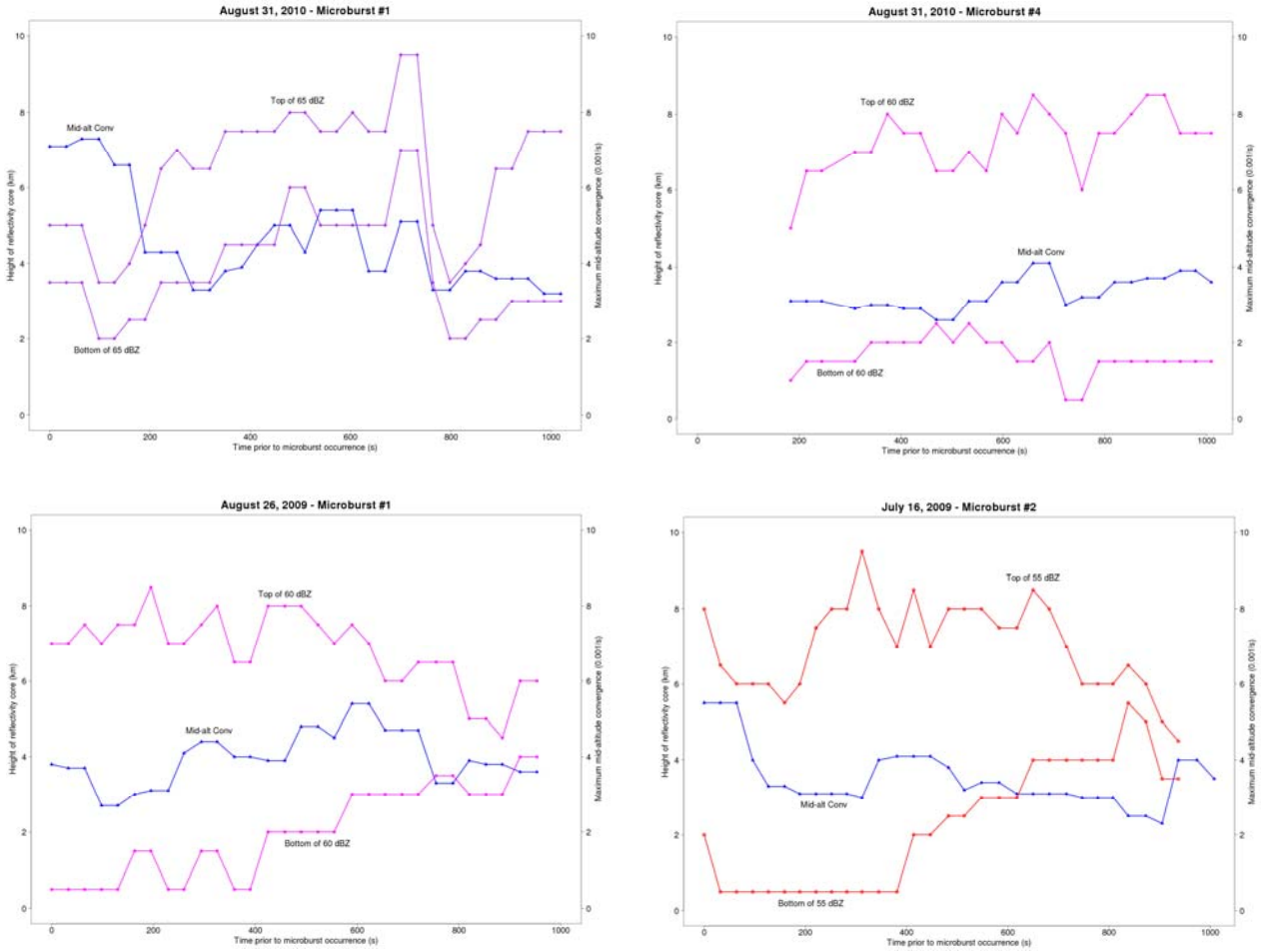

Figure 5. Time-series of the maximum mid-altitude convergence and the vertical extent of the precipitation core for the microburst-producing storms in Group 1. The reflectivity value chosen for displaying the character of the precipitation core is the one thought to be most representative of the downdraft forcing mechanisms associated with the storm (i.e., precipitation drag and cooling from melting ice).

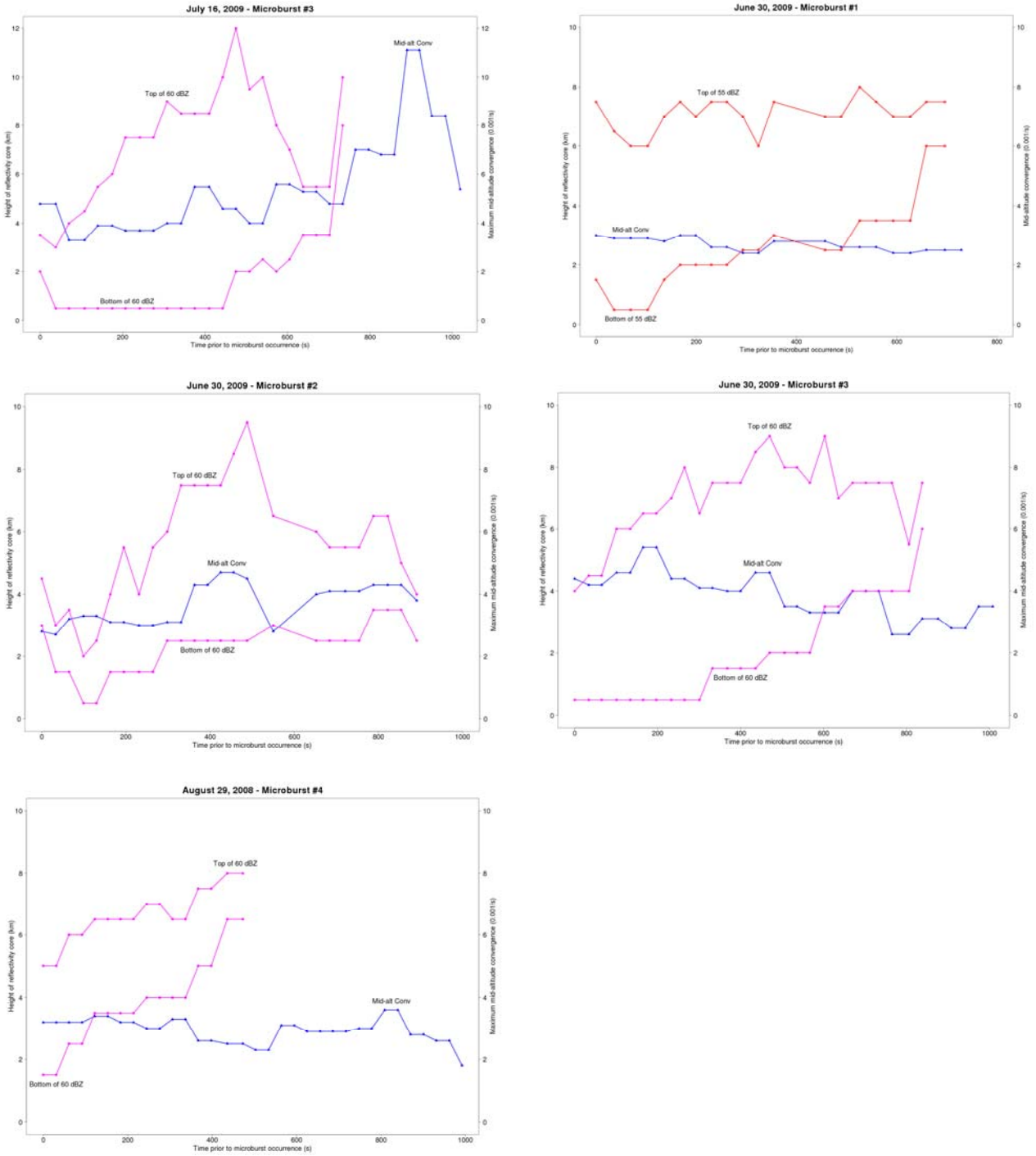

Figure 5 (continued).

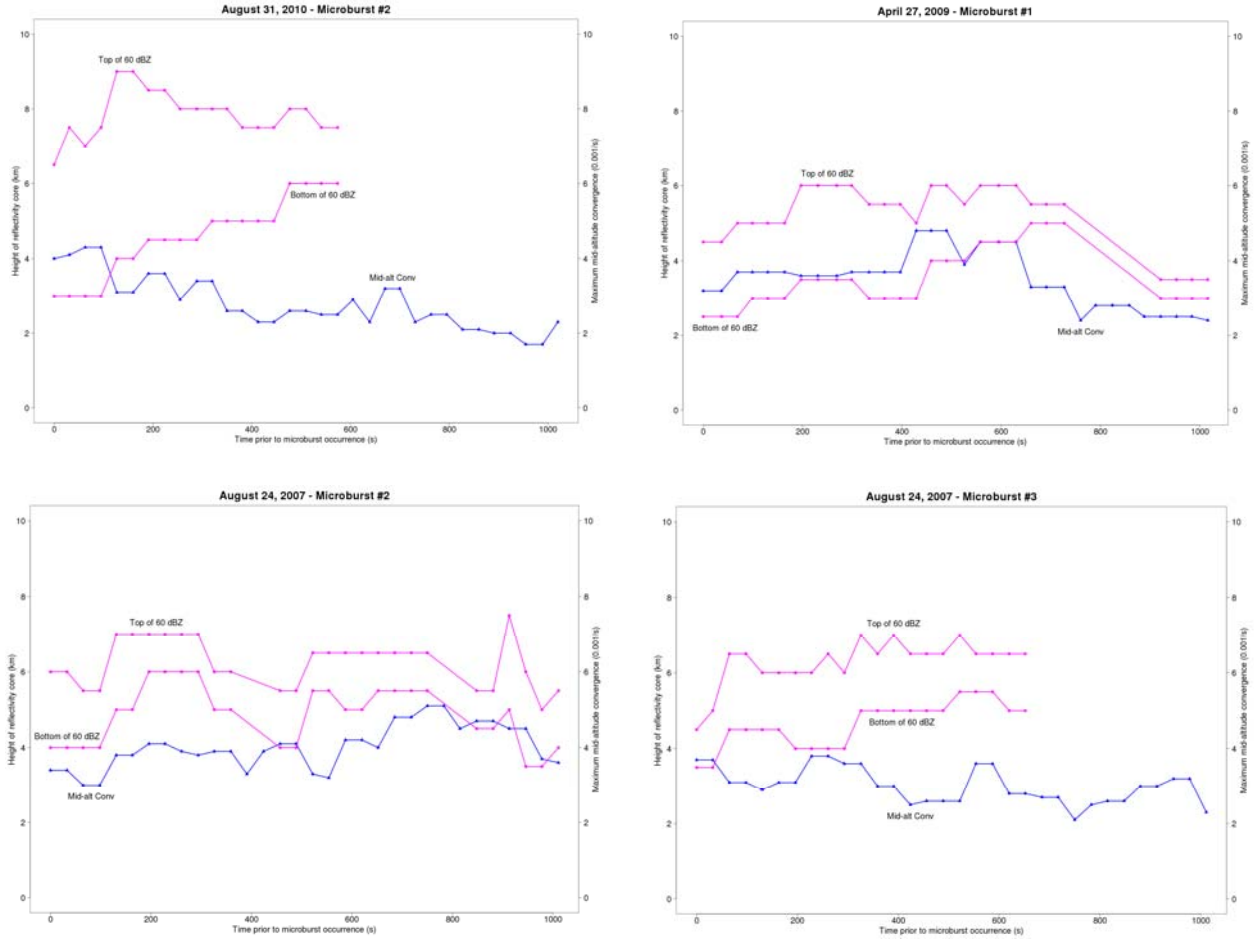

Figure 6. Same as Fig. 5, except for Group 2

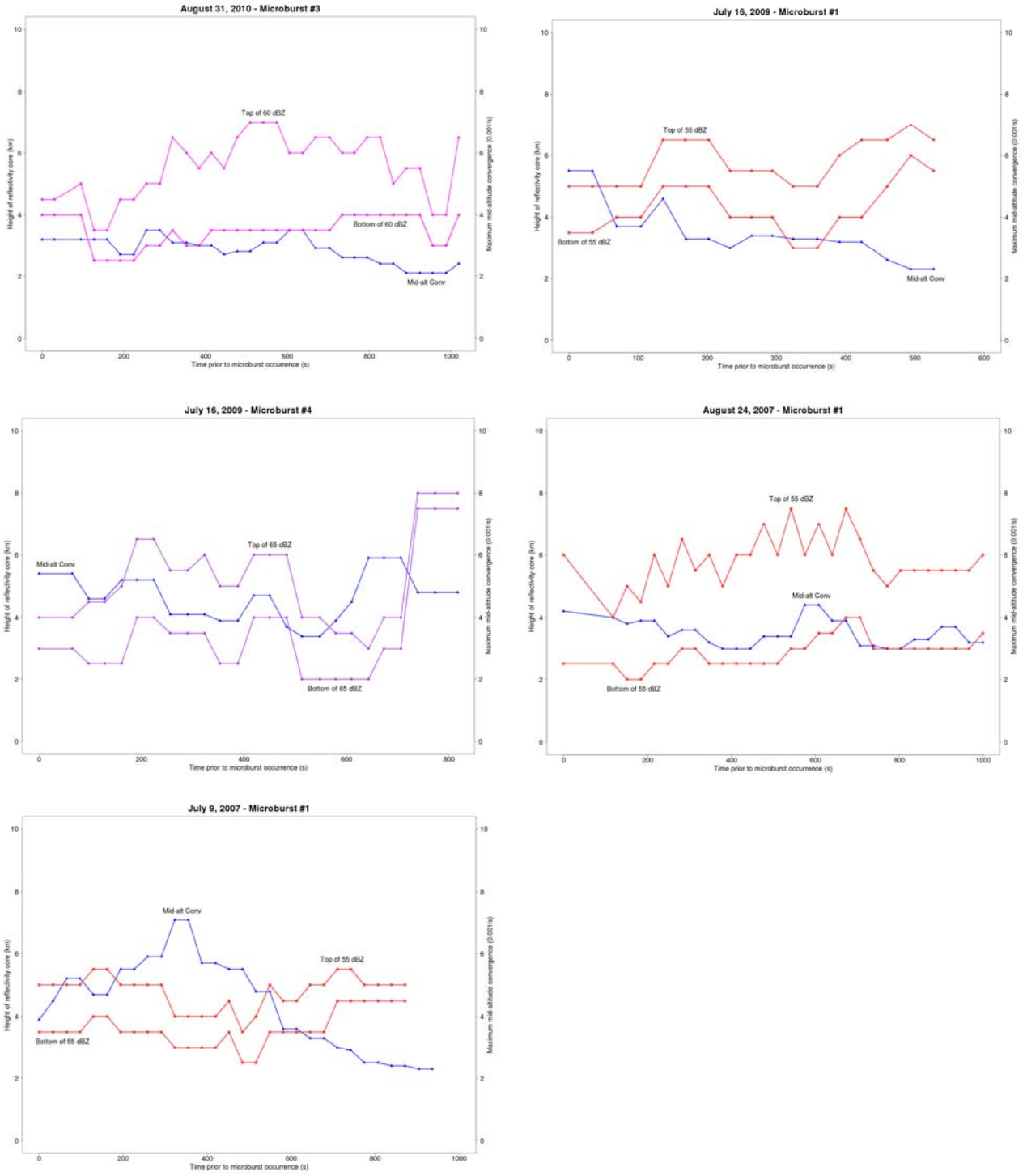

Figure 7. Same as Fig. 5, except for Group 3.

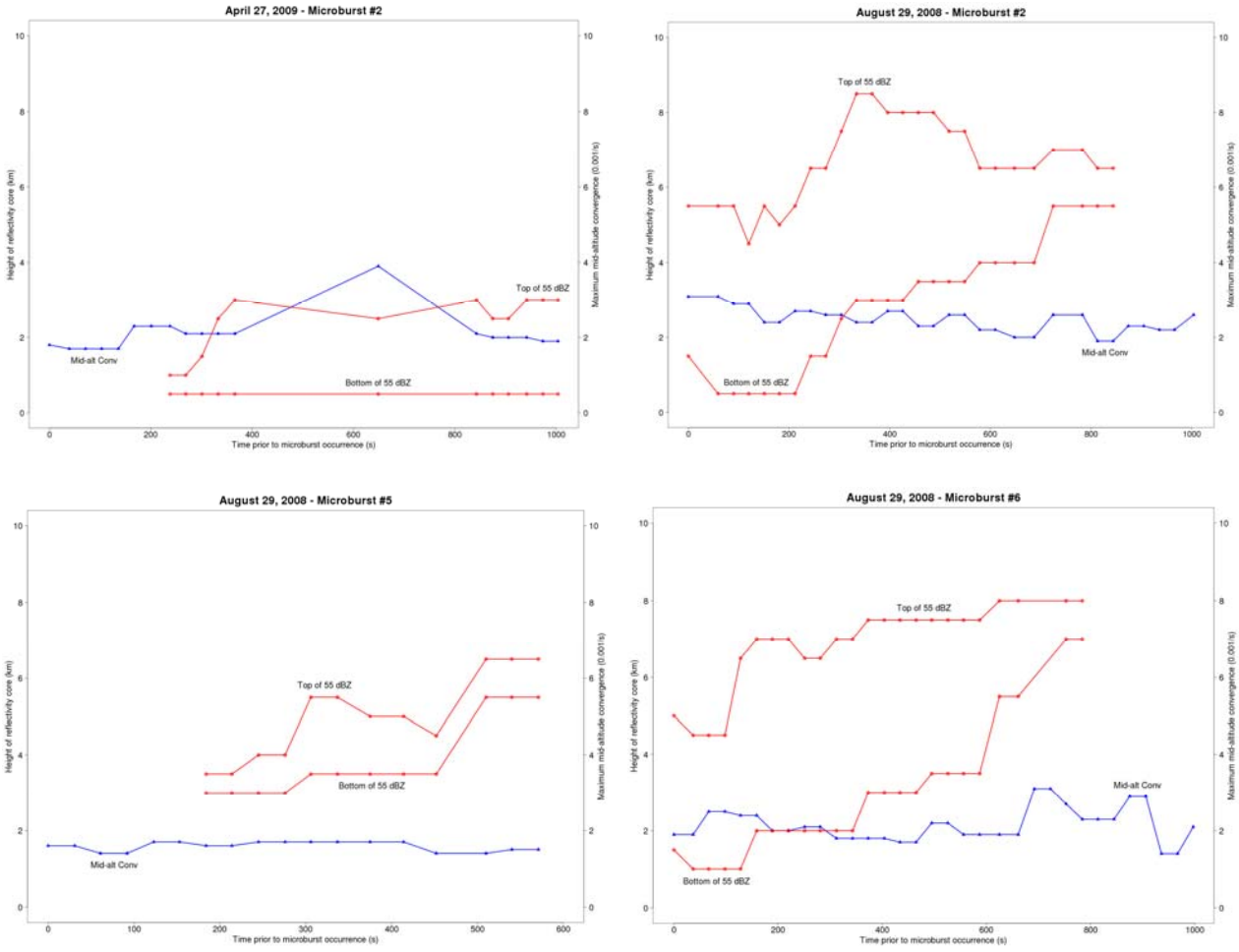

Figure 8. Same as Fig. 5, except for Group 4.

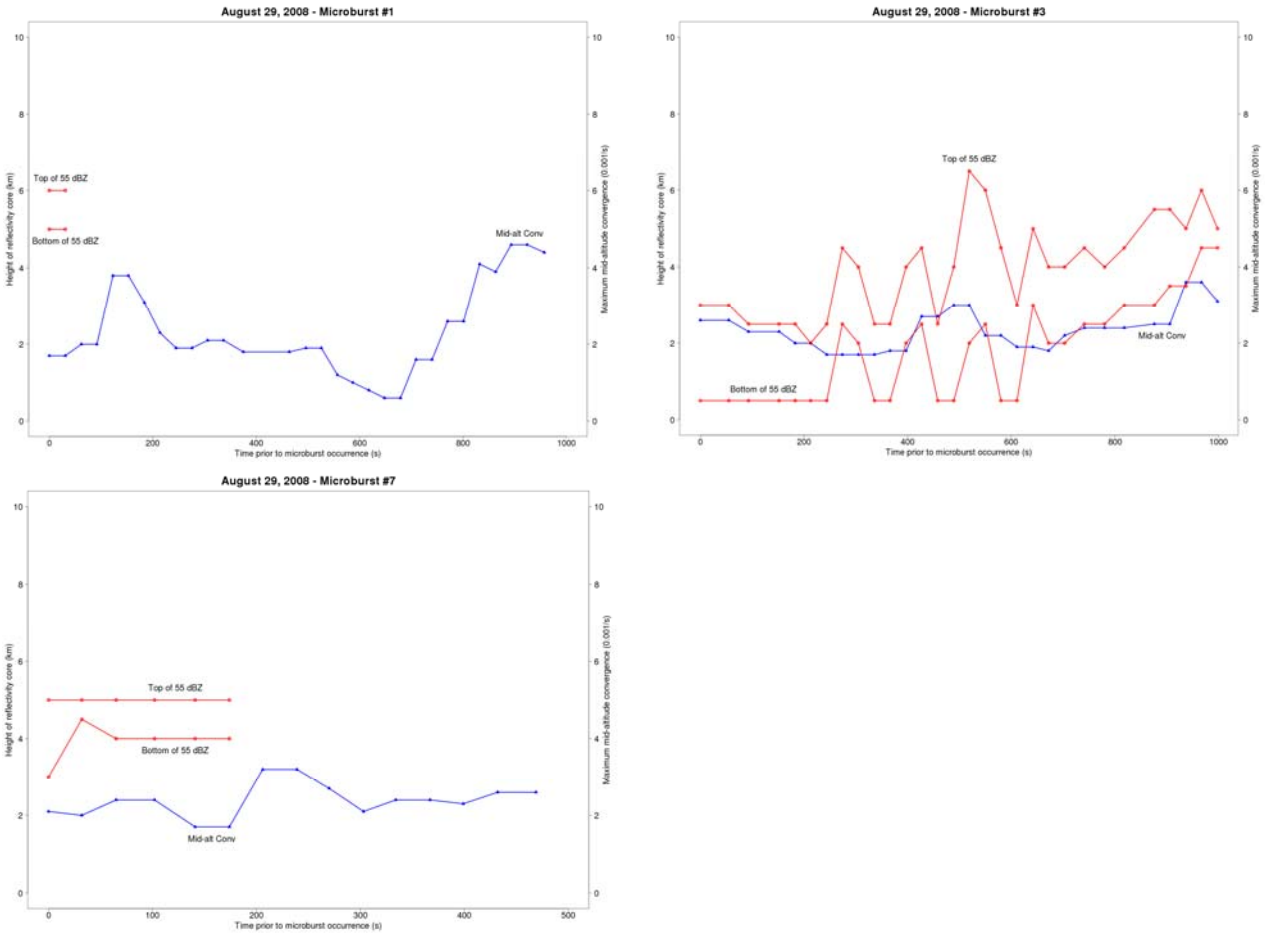

Figure 9. Same as Fig. 5, except for Group 5.